I&EC research
Industrial & Engineering Chemistry Research

Article

Cite This: Ind. Eng. Chem. Res. 2019, 58, 10524−10532

pubs.acs.org/IECR

Polybenzimidazole for Active Pharmaceutical Ingredient Purification: The Mometasone Furoate Case Study

Flávio Alves Ferreira,[†] Teresa Esteves,[†] Marta P. Carrasco,[‡] João Bandarra,[§] Carlos A. M. Afonso,[‡] and Frederico Castelo Ferreira*[,†,∥]

[†]iBB-Institute for Bioengineering and Biosciences, Department of Bioengineering and [∥]The Discoveries Centre for Regenerative and Precision Medicine, Lisbon Campus, Instituto Superior Técnico, Universidade de Lisboa, Avenida Rovisco Pais, 1049-001 Lisboa, Portugal

[‡]Faculty of Pharmacy, Universidade de Lisboa, Avenida Prof. Gama Pinto, Research Institute for Medicine (iMED, ULisboa), 1649-003 Lisboa, Portugal

[§]Hovione FarmaCiencia SA, R&D, Sete Casas, 2674-506 Loures, Portugal

Supporting Information

ABSTRACT: Active pharmaceutical ingredient (API) purity is of major concern for pharmaceutical companies and the medical community. Reaching ultralow limits of genotoxic impurities (GTIs), imposed by strict legislation, is often time consuming and economically challenging. Therefore, there is a call for efficient unit operations able to remove GTI with minimal API losses from the organic solvent postreactional streams. This study reports for the first time a new approach to improve the performance of polybenzimidazole (PBI), a solvent-stable polymer, to efficient GTI removal. Two families of GTIs are considered, and the discovery that the use of specific thermal and pH conditioning of PBI adsorbers improves GTI removal efficiency is reported. Electrospun fibers are explored, aiming at process versatility. Similar removals of GTI, more than 97%, are achieved with virtually no API loss.

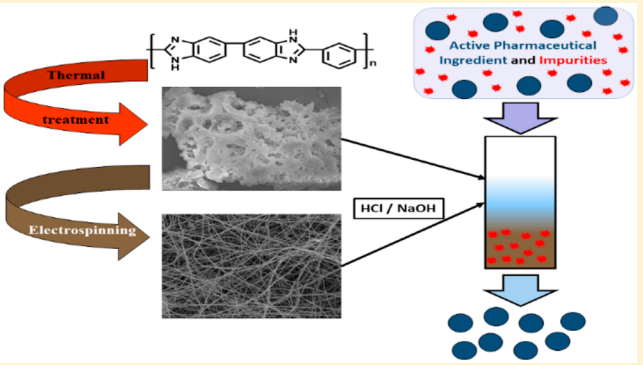

1. INTRODUCTION

The presence of genotoxic impurities (GTIs) in active pharmaceutical ingredients (APIs) is an issue of permanent concern for pharmaceutical companies and patients' well being.[1,2] Synthetic API production is mainly performed in organic solvent matrices using highly reactive species (e.g., reagents, catalysts) that may persist in the final formulations.[3] Strict regulatory measures impose a threshold of toxicological concern (TTC) limiting the presence of GTIs in APIs to a maximum of 1.5 μg/day.[4,5] To address this challenging low limit, several purification strategies have been extensively explored[6] including distillation, solvent exchange, recrystallization, and organic solvent nanofiltration (OSN) platforms[7−9] or the use of conventional[10] or tailor-made imprinted adsorbers.[11,12] However, since APIs are mainly obtained in organic solvent streams, the use of existing simple and efficient adsorbers is sometimes impaired or even impossible. In a previous report,[10] we addressed the purification of a corticosteroid API, Mometasone furoate (Meta), in the presence of two potential GTIs (4-dimethylaminopyridine, DMAP, and methyl *p*-toluenesulfonate, MPTS). Meta is used in the treatment of several inflammatory disorders[13] being possible to establish examples with administrations of 200 μg/day for airways treatment (e.g., allergic rhinitis and asthma) or 2 mg/day for topic use (e.g., eczema and psoriasis), corresponding to limits imposed by the TTC of 7.5 and 0.75 mgGTI/gAPI, respectively. In such study, the use of commercial resins was assessed for GTI removal and API recovery from methanol (MeOH) based recrystallization mother liquors. However, API synthesis usually includes the use of harsher chemical conditions and solvents than MeOH. In these situations, the use of commercial resins is no longer a suitable option, and the development of robust and versatile adsorbers still remains challenging. Polybenzimidazole (PBI) is an organic solvent compatible polymer that has been explored in the manufacturing of OSN membranes for API purification.[14−17] Recently, this polymer has been modified to bear adenine motifs in appending chains and has been assessed for the removal of several families of DNA alkylating GTI agents in dichloromethane (DCM) solutions with good results.[18,19]

Received: March 7, 2019
Revised: May 15, 2019
Accepted: May 24, 2019
Published: May 24, 2019

DOI: 10.1021/acs.iecr.9b01285
Ind. Eng. Chem. Res. 2019, 58, 10524−10532

In such previous reports, PBI was dissolved in dimethyl sulfoxide (DMSO) at high temperatures (>160 °C), ensuring its complete dissolution or/and mixing of reagents,[18,20] which led us to question if such heating step could have an effect on GTI adsorption, through induction of some structural or configurational features on PBI. Also, considering the chemical structure of unmodified PBI (Scheme 1), we decided to investigate in this work whether PBI adsorbers for GTIs could be developed using adequate thermal and/or pH conditioning. Therefore, this study provides a systematic assessment of such conditioned PBIs on their performance for GTI removal from API mixtures in an organic solvent. Moreover, in this report, a model system is considered comprising Meta as API and DMAP and MPTS as model GTIs.

Scheme 1. Proposed Interaction Mechanisms between PBI-TA and DMAP (top) and PBI-TB and MPTS (bottom)

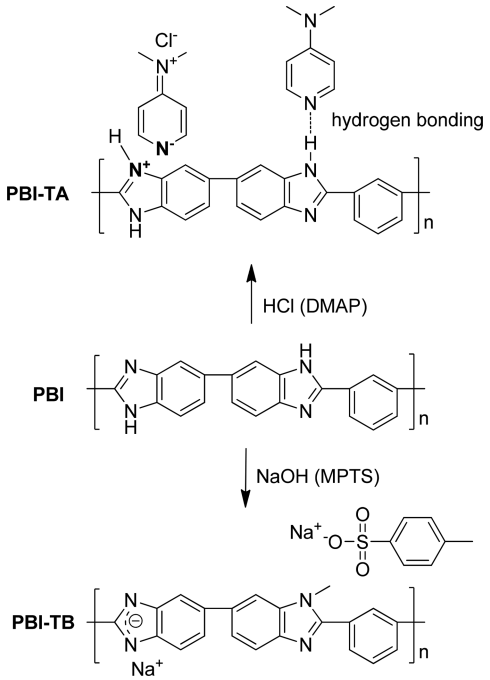

2. MATERIALS AND METHODS

2.1. Materials. 4-Dimethylaminopyridine (DMAP), methyl *p*-toluenesulfonate (MPTS), and *p*-toluenesulfonic acid monohydrate (PTSA) were purchased from Acros (Belgium). Pristine polybenzimidazole (PBI) polymer 100 mesh powder was purchased from PBI Performance Products Inc. (USA). PBI was selected because it combines two features: it is a polymer stable in a wide range of solvents and high temperatures, and its chemical-physical properties allow one to establish different types of noncovalent bonds to be used in adsorption, namely, hydrogen, pi−pi, electrostatic, and ionic bonds. All of these reagents were used as supplied without further purification. Dichloromethane (DCM), methanol (MeOH), and acetonitrile (MeCN) HPLC-grade solvents, toluene (MePh), ethyl acetate (EtOAc), hydrochloric acid (HCl) 37% solution, and sodium hydroxide (NaOH) pellets were purchased from Fisher Chemicals (USA). Dimethyl sulfoxide (DMSO) was purchased from Carlo Erba (Spain). Formic acid (FA) and dimethylacetamide (DMAc) were purchased from Panreac (Spain). Mometasone furoate (Meta) and betamethasone acetate (Beta) were kindly provided by Hovione PharmaScience Ltd. (Portugal).

2.2. Apparatus and Analysis. Nitrogen adsorption isotherms were obtained at 77 K in adsorption apparatus (ASAP 2010 Micromeritics), and the samples were degasified at 80 °C for 16 h. HPLC measurements of the analytes were performed on a Merck Hitachi pump coupled to a L-2400 tunable UV detector using an analytic Macherey-Nagel C18 reversed-phase column Nucleosil 100−10, 250 × 4.6 mm. The volume of injection was 10 μL, and the eluents were an aqueous 0.1% FA solution (eluent A) and MeCN 0.1% FA solution (eluent B). For MPTS: flow rate of 2 mL·min^{-1}; UV detection at 230 nm; method: 0−15 min, 70% A. For PTSA: flow rate of 1.5 mL·min^{-1}; UV detection at 230 nm; method: 0−10 min, 90% A. For DMAP, Meta, and Beta: UV detection at 280 nm; flow rate of 1 mL·min^{-1}; method: 0−3 min, 60% A; 3−4 min, 20% A; 4−8 min, 20−60% A; 8−15 min 60% A. SEM experiments were performed on a FEG-SEM (field emission gun-scanning electron microscope) from JEOL, model JSM-7001F, with an accelerating voltage set to 15 kV. Samples were mounted on aluminum stubs using carbon double-sided tape and were coated with a 20 nm gold/palladium (80/20) film on a Quorum Technologies Sputter Coater, model Q150T ES.

2.3. PBI Polymer Processing. PBI thermal treated (**PBI-T**) was obtained by dissolving pristine PBI polymer in DMSO (15% w/w) by heating, under air, at 163 °C for 3 h with magnetic stirring. The solution was then cooled to 50 °C and precipitated with water. The resulting solid was crushed, filtered, and successively washed with water (40 mL/g polymer), MeOH (20 mL/g polymer), and DCM (20 mL/g polymer) for 3 min each with magnetic stirring (3 times for each solvent). The solid obtained was then dried under vacuum.

To perform the pH conditioning of PBI adsorbers, pristine PBI polymer and **PBI-T** were pH conditioned with HCl 0.25 M (**PBI-A** and **PBI-TA**) or NaOH 0.1 M (**PBI-B** and **PBI-TB**) solutions by washing. The polymers were immersed for 3 min in 20 mL of acidic or basic solution per gram of polymer with magnetic stirring. After this the polymers were successively washed by magnetically stirring for 3 min in solutions of water (40 mL/g polymer), MeOH (20 mL/g polymer), and DCM (20 mL/g polymer) (3 times for each solvent) and dried under vacuum overnight. The polymers were removed from each solution by simple filtration and transferred to the next solvent.

2.4. GTI Binding Experiments. Batch binding experiments were performed by placing 50 mg of each polymer in 2 mL Eppendorf vials and addition of 1 mL of a solution of each GTI (DMAP, MPTS) alone or in combination with each API (Meta, Beta) prepared in solvent at concentrations of 100, 1000, and 5000 ppm for the GTIs or 10 000 ppm for the APIs. The suspensions were stirred for 24 h at 200 rpm. After this time the samples were centrifuged for 3 min at 10 000 rpm, and the supernatant was filtered and analyzed by HPLC for GTI and API quantification. These assays were performed with duplicate samples against controls. The same procedure was performed using 10 mg of fibers, in 1 mL sample volume, with API and GTI mixtures in DCM. Except when stated otherwise, the solvent used was DCM.

The percentage of GTI or API bound to the adsorbers was calculated from eq 1

DOI: 10.1021/acs.iecr.9b01285
Ind. Eng. Chem. Res. 2019, 58, 10524−10532

$$\text{binding}\ (\%) = \frac{[C_0 - C_f]}{C_0} \times 100 \quad (1)$$

where C_0 (mg/L) is the initial GTI or API concentration and C_f (mg/L) is the final GTI or API concentration in solution.

The amount of GTI or API bound to the adsorbers was calculated from eq 2

$$Q = \frac{V \times [C_0 - C_f]}{M} \quad (2)$$

where Q (mg/g) is the amount of GTI or API bound to the adsorber, C_0 (mg/L) is the initial GTI or API concentration, C_f (mg/L) is the final concentration of GTI or API in solution, V (L) is the volume of solution used, and M (g) is the adsorber mass.

2.5. Binding Adsorption Isotherm Experiments. For the adsorption isotherm experiments at room temperature, 1 mL of DMAP, MPTS, or Meta solutions prepared in DCM, with different initial concentrations, from 100 ppm to 10 000 ppm, was added to 50 mg of the adsorbers. The mixtures were stirred at 200 rpm for 24 h. After that time the suspensions were centrifuged and the supernatants were filtered and analyzed by HPLC. All experiments were carried out in duplicate. The percentage and the amount of GTI or API bound to the adsorbers were calculated from eqs 1 and 2. The experimental data were fitted to the Langmuir and Freundlich isotherm models[21] according to eqs 3 and 4, respectively

$$\frac{q_f}{q_m} = \frac{K_L C_f}{1 + K_L C_f} \quad (3)$$

$$q_f = K_F C_f^{1/n} \quad (4)$$

where q_m (mg/g) is the maximum amount of GTI bound to the adsorber in a monolayer for the Langmuir model, whereas K_L and K_F are equilibrium constants (L/mg) for the Langmuir and Freundlich models, respectively, and are related with the energy taken for adsorption; n is a parameter related with the surface layer heterogeneity.

To compare the validity of each model, chi square (χ^2) was assessed, according to eq 5, since correlation coefficient (R^2) may not justify the selection of the most suited adsorption model because it only translates the fit between linear forms of the model equations and experimental data, while the suitability between experimental and predicted values of the adsorption capacity is described by chi square (χ^2). The lower the χ^2 value, the better the fit.[22]

$$\chi^2 = \sum \frac{(\text{predicted data} - \text{experimental data})^2}{\text{predicted data}} \quad (5)$$

2.6. Binding Kinetics Experiments. The adsorption kinetics studies were performed at room temperature for DMAP, while for MPTS they were performed at room temperature and 50 °C. After certain time intervals (5, 10, 15, 30, 45, 60, 120, 240, 360, 480, and 1440 min) 1000 ppm solutions prepared in DCM, left stirring at 200 rpm, were analyzed. At these times, the suspensions were centrifuged, and the supernatants were filtered and analyzed by HPLC. All experiments were carried out in duplicate. The percentage and the amount of GTI bound to the adsorber were calculated from eqs 1 and 2. The experimental data were fitted to pseudo-first- and pseudo-second-order kinetic models[23] according to eqs 6 and 7, respectively

$$\ln(q_f - q_t) = \ln(q_f) - k_1 t \quad (6)$$

$$\frac{t}{q_t} = \frac{1}{k_2 . q_f^2} + \frac{t}{q_f} \quad (7)$$

where q_f and q_t (mg/g) are the adsorption capacities at the final and time t (min), respectively, and k_1 (min^{-1}) and k_2 (g/(mg·min)) are the pseudo-first-order and second-order rate constants for the models.

To compare the validity of each model, chi square (χ^2) was assessed, following eq 5, since correlation coefficient (R^2) may not justify the selection of the most suited binding kinetic model because it only translates the fit between linear forms of the model equations and experimental data, while the suitability between experimental and predicted values of the kinetic studies is described by chi square (χ^2). The lower the χ^2 value, the better the fit.[24]

2.7. API Recovery Experiments. For Meta recovery, after binding experiments, the adsorbers, **PBI-TA** and **PBI-TB**, were washed with 1 mL of DCM for 24 h at 200 rpm, centrifuged, and the supernatant was analyzed by HPLC. After that, for GTI removal from **PBI-TA** or **PBI-TB**, the polymers were washed with 1 mL of MeOH for 24 h at 200 rpm and centrifuged, and the supernatants were analyzed by HPLC. Meta recovery and GTI removal were calculated by simple percentage.

2.8. Electrospinning Setup. Fibers were prepared for a 13 wt % PBI solution in DMAc. The electrospinning process was carried out at 30 kV with a steady flow of 0.3 mL·h^{-1} in a homemade set up previously described.[25] A needle with 0.51 mm of internal diameter was used, and the electrospun fibers were collected on an aluminum target at a distance of 16 cm from the needle. The fibers obtained were subjected to pH conditioning by immersion in HCl 0.25 M or NaOH 0.1 M solutions for 3 min (20 mL of solution per gram of polymer, with occasional stirring). After this the fibers were successively washed for 3 min in water (40 mL/g polymer), MeOH (20 mL/g polymer), and DCM (20 mL/g polymer) (3 times for each solvent) and dried under vacuum overnight. The fibers were removed from each solution by decantation and transferred to the next solvent.

3. RESULTS AND DISCUSSION

In this report we study whether a dissolution step, at high temperature, and different ionic states of PBI polymer, similarly to ionic exchange resins, could be explored to confer improved adsorption properties to PBI. PBI can be found in different protonation states according to its pK_a (5.23).[26,27] The imidazole ring present in PBI structure can act either as an electron acceptor or as an electron donor and be present in different protonation states depending on the pH. Therefore, the initial pristine PBI was subjected to a thermal treatment (**PBI-T**) or/and acidic (**PBI-A**/**PBI-TA**) and basic (**PBI-B**/**PBI-TB**) pH conditioning to verify the optimal properties that could improve impurity removal, from solution, at the expense of the lowest API losses.

3.1. Screening PBI Adsorbers for GTI Removal. The performance of the new adsorbers, **PBI-T**, **PBI-A**, **PBI-B**, **PBI-TA**, and **PBI-TB**, was assessed against solutions of GTIs (DMAP or MPTS) alone or in combination with an API (Meta) in DCM (Figure S1). From the results presented in Figure 1 it was possible to observe that **PBI-T**, with thermal treatment, induces a better performance for GTI removal (40–

DOI: 10.1021/acs.iecr.9b01285
Ind. Eng. Chem. Res. 2019, 58, 10524−10532

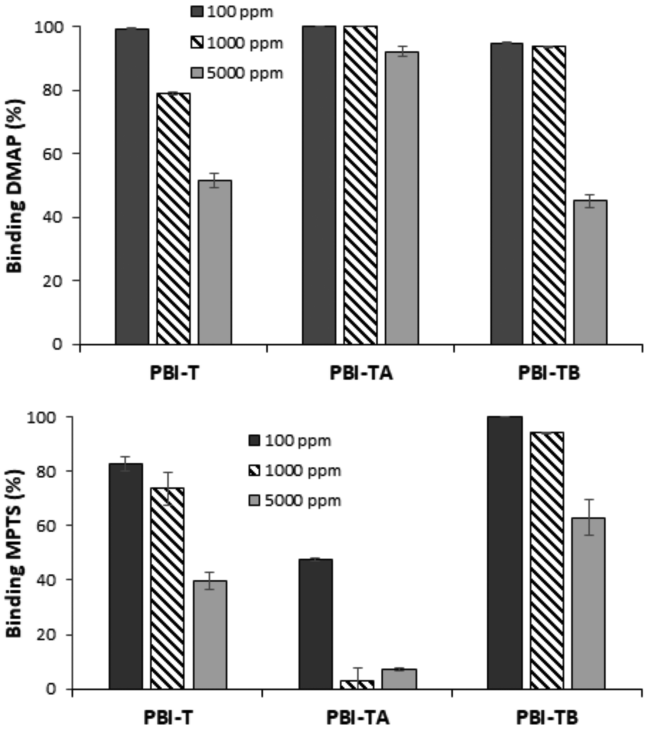

Figure 1. (Top) DMAP binding for 100, 1000, and 5000 ppm solutions in DCM for different PBI adsorbers. (Bottom) MPTS binding for 100, 1000, and 5000 ppm solutions in DCM for different PBI adsorbers.

99%) comparing with pristine PBI polymer (2−14%). Moreover, coupling this feature to specific pH conditioning improves, according with GTI nature, even further this performance for highly concentrated GTI solutions above 1000 ppm. For this reason, **PBI-TA** and **PBI-TB** were the adsorbers selected to be further explored in the remaining studies reported in this work.

In the specific case of DMAP, for a solution concentration of 1000 ppm, both **PBI-TA** and **PBI-TB** are effective with removals higher than 93%. However, when the concentration is increased to 5000 ppm, only **PBI-TA** remains effective (92%) while **PBI-TB** removal decreases by one-half (45%), remaining at the same level of DMAP removal achieved by **PBI-T**, at this concentration. For this reason, **PBI-TA** polymer was selected to address DMAP scavenging. DMAP can interact with pristine PBI through hydrogen bonding between the nitrogen of the aromatic ring and the amine groups present in the benzimidazole rings of PBI. However, DMAP also presents a dipolar resonance allocating the negative charge on the nitrogen of the aromatic ring,[28] which can favor an ionic interaction with the protonated groups of **PBI-TA** (Scheme 1). Synergistically, both of these interactions may improve DMAP binding for **PBI-TA** for concentrations higher than 1000 ppm as was observed.

In the case of MPTS, **PBI-TB** always presented a higher performance (63−97%) in removing this impurity when compared to **PBI-TA** (7−47%). A significant improvement of the basic treatment was obtained with higher MTPS removals for **PBI-TB** when compared with **PBI-T**; however, the acid treatment resulted in lower MPTS removals by **PBI-TA**. For this reason, **PBI-TB** polymer was considered the more suited adsorber to treat solutions containing this GTI. In the case of this impurity, the interaction with PBI is expected to follow a methylation reaction of the amine groups of the imidazole rings of the adsorber, as observed previously for a **PBI-adenine**-modified polymer.[18,19] However, further deprotonation of PBI in the presence of NaOH, originating **PBI-TB**, favors this reaction, with the sodium ions stabilizing the anion of MPTS, as represented in Scheme 1.

The effect of the solvents on model PGTI adsorption was assessed for solutions of 1000 ppm (Figure S2), achieving bindings higher than 65% for MPTS (adsorption on **PBI-TB**) and 90% for DMAP (adsorption on **PBI-TA**) with exceptions for water and MeOH with DMAP adsorptions of 4.5% and 10%, respectively. The lower adsorption for these two polar solvents can be attributed to possible competition of the solvent by the polymer binding sites, since the proposed adsorption mechanism for DMAP is through hydrogen bonds. This feature can be employed to perform the removal of DMAP bound to **PBI-TA**. MPTS bindings were higher than 90% for AcOEt, MeCN, and DCM, showing that PBI can be used to remove this GTI from solvents of different chemical families.

3.2. Adsorbers Characterization. Nitrogen gas adsorption was used to estimate BET surface area, the total pore volume, and the pore size for the different adsorbers (Table 1).

Table 1. Physical Properties of Pristine PBI and Several PBI-Derived Adsorbers Obtained by the Multipoint BET Method[a]

	BET surface area ($m^2 \cdot g^{-1}$)	pore volume ($cm^3 \cdot g^{-1}$)	pore diameter (Å)
pristine PBI	n.d.[b]	n.d.	n.d.
PBI-T	28.31	0.19	299.55
PBI-A	n.d.[b]	n.d.	n.d.
PBI-B	n.d.[b]	n.d.	n.d.
PBI-TA	27.77	0.18	309.35
PBI-TB	33.26	0.21	308.90
f-**PBI-TA**	13.52[c]	0.03	90
f-**PBI-TB**	17.72[c]	0.03	66

[a] *f* − fiber; n.d. − not determined. [b] Nonporous or microporous material (below detection limit of 4 $m^2 \cdot g^{-1}$). [c] Values obtained using $p/p_0 < 0.1$, as there is a lack of linearity for values above $p/p_0 > 0.1$. Mercury intrusion porosimetry was also used to obtain a surface area of 13.19 and 16.44 $cm^2 \cdot g^{-1}$, respectively, for **PBI-TA** and **PBI-TB** fibers.

Only for the polymers subjected to thermal treatment (**PBI-T**, **PBI-TA**, **PBI-TB**), it was possible to record the different parameters with all polymers showing similar properties. For the remaining polymers, due to the lower surface area, the isotherms showed an irregular behavior, not allowing one to calculate BET parameters for these samples. This can be due to surface modification of the particles that occurs during polymer precipitation in water, acting as a cosolvent, in a process similar to phase inversion that is used in the casting of PBI membranes.[29] This observation is supported by SEM images showing the presence of a smooth surface for pristine PBI, **PBI-A**, and **PBI-B** particles (Figure S3), contrasting to a rough porous surface for **PBI-T**, **PBI-TA**, and **PBI-TB** particles (Figure 2).

From the SEM images it is clear that the formation of a more open and porous structure for beads obtained after thermal treatment involves the dissolution of PBI at high temperatures in DMSO than for pristine PBI beads. Although **PBI-TA** and **PBI-TB** presented a good binding toward the

DOI: 10.1021/acs.iecr.9b01285
Ind. Eng. Chem. Res. 2019, 58, 10524−10532

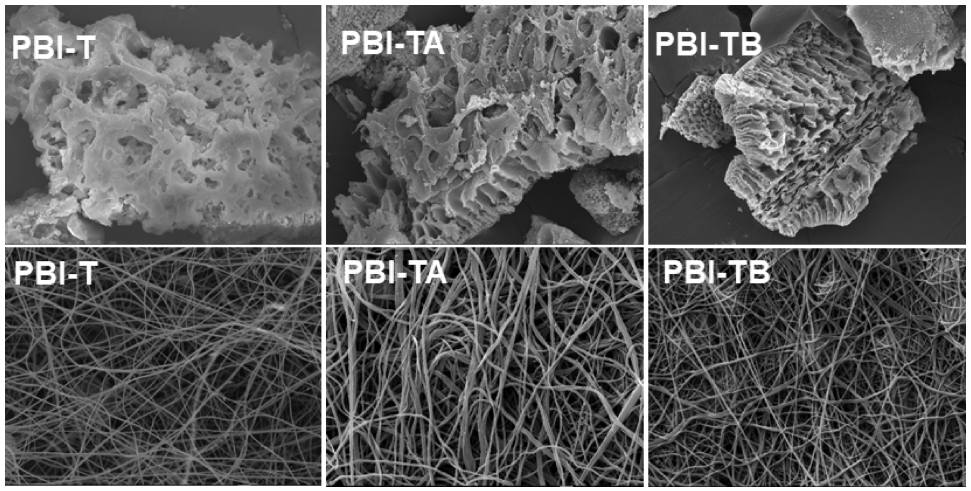

Figure 2. SEM images of PBI polymer particles and fibers. (Top) Beads obtained after thermal treatment. (Bottom) Electrospun fibers obtained from thermal-treated PBI.

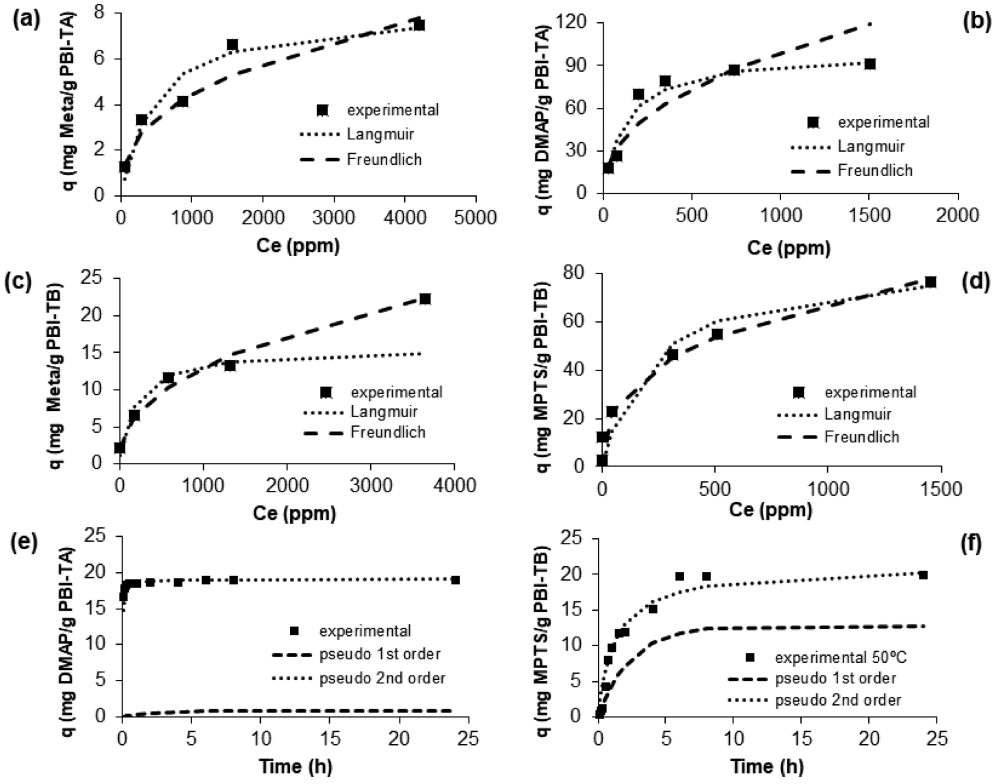

Figure 3. (Top) Binding isotherm fitting models for DMAP (b) and Meta (a) for **PBI-TA** at room temperature. (Middle) Binding isotherm fitting models for MPTS (d) and Meta (c) for **PBI-TB** at room temperature. (Bottom) Kinetic fitting models for DMAP and **PBI-TA** at room temperature (e) and MPTS and **PBI-TB** at 50 °C (f).

GTIs, each adsorber targets only one of the species preferentially (**PBI-TA** for DMAP and **PBI-TB** for MPTS). This result indicates that the interaction behind GTI recognition is not only governed by the surface area of the polymeric particles, relying instead in specific ionic or covalent interactions established between the adsorbers, in a specific ionic state, and the GTI molecules, as discussed in section 3.1. Furthermore, SEM images (Figure 2) show that the electrospun fibers obtained are randomly deposited and have an average diameter of (146.92 ± 19.96) nm (Figure S4), and their morphology is not affected after pH conditioning, maintaining their integrity.

3.3. Binding Isotherm and Kinetic Studies. As can be seen from the adsorption binding experiments shown in Figure 3, DMAP and Meta follow the Langmuir model on **PBI-TA** with the formation of a monolayer with maximum adsorption of 100 mg of DMAP (and 8.22 mg of Meta) per gram of adsorber, whereas MPTS and Meta follow the Freundlich model on **PBI-TB** (Figure 3) following adsorption on multilayers. Physical parameters determined for both adsorbers, **PBI-TA** and **PBI-TB**, are presented in Table S1.

DMAP adsorption on **PBI-TA**, at room temperature, is fast reaching equilibrium after only 30 min with more than 97% binding of GTI following a pseudo-second-order model

DOI: 10.1021/acs.iecr.9b01285
Ind. Eng. Chem. Res. 2019, 58, 10524−10532

(Figure 3). In the case of MPTS with **PBI-TB**, the adsorption process, at room temperature, is slower with the equilibrium being reached within 24 h following a pseudo-second-order kinetics (data not shown). In this case, **PBI-TB** presents higher surface area compared to pristine PBI and more accessible nucleophilic nitrogen atoms compared to **PBI-TA**, allowing for, respectively, $\pi-\pi$ interaction between polymer and MPTS and nucleophilic substitution of the amine imidazole polymer ring. Such suggested mechanisms are slower than ionic interactions, which would be consistent with lower binding kinetics observed. Experiments performed at 50 °C showed that these interactions are favored with temperature, with the equilibrium being reached within just 2 h following a pseudo-second-order kinetic model (Figure 3). Kinetic physical parameters for **PBI-TA** and **PBI-TB** are presented in Table S2. Overall, for both GTIs, the kinetic profile observed is concentration dependent with different k_2 values, as observed for experiments performed for 100 and 1000 ppm (Figure S5 and Table S3).

3.4. API Purification Studies. In sections 3.1 and 3.2, adsorption for single-solute solutions, containing API or GTIs alone, was evaluated. However, for solutions containing both API and GTI, a possible competition between the species for available binding sites of adsorber may take place, possibly affecting the binding of different species. In order to assess this solutions simulating an API post reaction stream in DCM with 10 000 ppm of API and 1000 ppm of GTI were assessed with **PBI-TA** and **PBI-TB** (Figure 4).

For DMAP and **PBI-TA**, no difference was observed for GTI removals (around 99%) using single-solute solutions or mixtures of GTI and API. For the APIs, Meta adsorption on **PBI-TA** remained lower than 10%, and for Beta the adsorption remained around 20%, showing that this adsorber performance was not affected by the presence of both species in solution.

However, for MPTS in **PBI-TB** at room temperature, there was a significat reduction of GTI removal, from 94% to 50%, followed by an increase in APIs adsorption, from around 9% to around 25% when both compounds were mixed in solution.

Changes in API concentration are assumed to be allocated only to adsorption, as in previous studies it was established that there was no interaction between MPTS and API[10] and supported by mass balance for API recovered from the adsorber (Table 2).

Betamethasone acetate (Beta), also a glucocorticoid-like Meta, was tested to verify if the results obtained for **PBI-TB** were only due to the presence of Meta. These APIs, although presenting the same general structure, contain different chemical functionalities that may impair or not the interaction with the adsorbers. Both APIs present halogen atoms at the 9α position with a chlorine for Meta and a fluorine for Beta. Moreover, at position 21 Meta has an additional chlorine atom, and at position 17 it has a furoate group, whereas Beta presents an ester group at position 21 and a hydroxyl group at position 17. Despite these structural differences, for **PBI-TB**, the same trend was observed for both glucocorticoids, with a lower efficiency in GTI removal and an increment in API loss for mixtures of MPTS and APIs than for single-solute assays. At this point, following the same reasoning of the binding kinetic studies and in order to solve this drawback, these experiments were also performed at 50 °C (Figure 4). With the increase in temperature, it was possible to observe that GTI removal was reestablished to previous values above 96% with API binding to the adsorber of only around 9%. MPTS binding to **PBI-TB** includes a methylation reaction, which is favored with temperature.

The use of PBI electrospun fibers is well established in the literature for applications in proton-conductive membranes.[30,31] Moreover, the use of fiber meshes allows for diverse process configurations, such as membrane contactors and adsorbers.[32,33] As illustrated in the SEM images, when PBI is electrospun, uniform and regular structures are obtained. Adsorption of GTIs and API were assessed for GTI and API mixtures using 10 mg of **PBI-TA** beads or fibers at room temperature and **PBI-TB** beads or fibers at 50 °C in 1 mL of DCM. Note that suboptimal amounts of 10 mg/mL of adsorber were used to perform experiments in conditions below the 100% GTI removal observed when using 50 mg/mL of beads. The reasoning for this is that the use of 10 mg/mL of polymer (instead of 50 mg/mL) avoids fiber compaction in the 1 mL test solution and allows for experimental detection of potential differences between fiber and beads adsorption performance.

DMAP removal in **PBI-TA** was slightly higher for the fibers, although not statistically significant (p = 0.12), than for beads (Figure 5). Concerning API loss, it was similar and around 20%. In the case of MPTS with **PBI-TB**, the API loss followed the same trend (around 10%) with a similar MPTS removal (p = 0.40) of around 50%. The surface area of the fibers is about one-third of the beads for the same weight of material (Table 1). However, the binding performance is similar (Figure 5), which can be explained by the more opened structure of the fiber meshes (Figure 2), offering to facilitate molecule access to the adsorption surface.

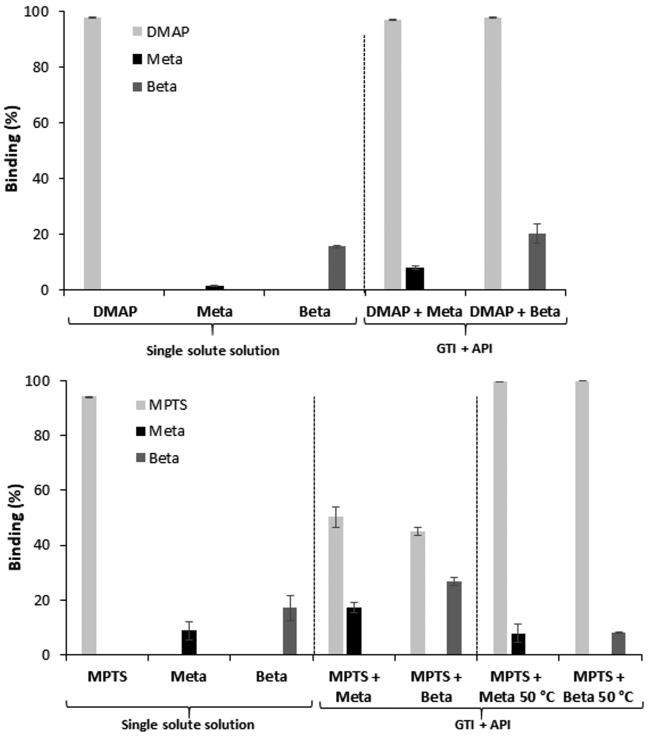

Figure 4. (Top) Comparison of adsorption of solutions of isolated API, isolated DMAP, and API+DMAP with **PBI-TA** at room temperature. (Bottom) Comparison of adsorption of solutions of isolated API, isolated MPTS, and API+MPTS with **PBI-TB** at room temperature and at 50 °C.

DOI: 10.1021/acs.iecr.9b01285
Ind. Eng. Chem. Res. 2019, 58, 10524−10532

Table 2. API Loss and mgGTI/gAPI Using PBI-TA for DMAP Removal and PBI-TB for MPTS Removal in a Meta Solution

	recovery (%)				after adsorption		after DCM washing	
	DCM		MeOH					
	Meta	GTI	Meta	GTI	mgGTI/gAPI	API loss (%)	mgGTI/gAPI	API loss (%)
PBI-TA	100	1.03	100	80.39	2.95	1.62	3.90	0
PBI-TB	100	<0.5	83.35	<0.65	<0.27	7.93	<0.25	0

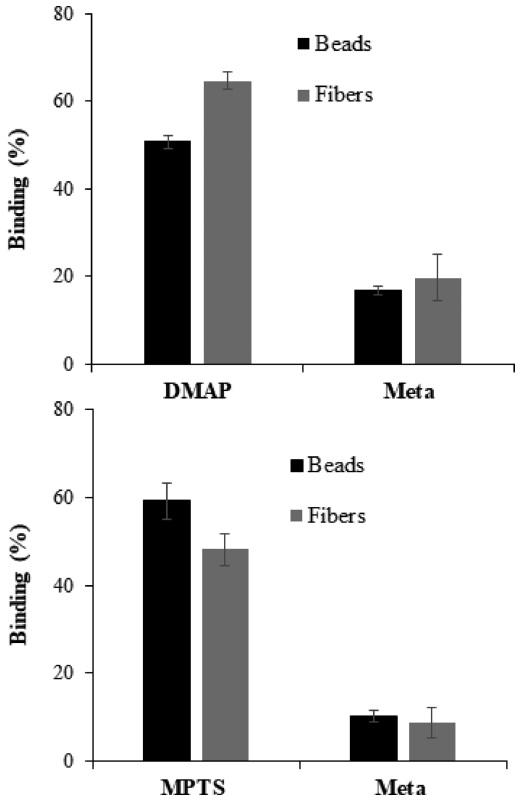

Figure 5. Comparison between binding performance of beads and fibers. (Top) **PBI-TA** for DMAP and Meta at room temperature. (Bottom) **PBI-TB** for MPTS and Meta at 50 °C.

These preliminary experiments suggest that, independently of the morphology of the adsorber, the physicochemical characteristics conferred to the material remained similar. This fact is important in applications requiring the use of electrospun fiber meshes such as in membrane separation processes to perform purification of APIs in organic solvent matrices.

Since PBI beads and fibers showed a similar behavior in solution, recovery of the API that remained bound to the adsorbers was only assessed for the beads. In order to reduce API loss, a recovery step was performed by assessing Meta desorption from the adsorbers using DCM or MeOH. Virtually all of the API was recovered from both polymers, **PBI-TA** and **PBI-TB**, after a simple first DCM washing (Table 2). In the case of **PBI-TA**, a minimum DMAP back contamination (around 1% of adsorbed GTI) was observed. When, alternatively, **PBI-TA** was first washed with MeOH, the API could also be fully recovered but with 80% of DMAP contamination (Table 2). Therefore, it is here suggested to use a first DCM washing for API recovery followed by a MeOH washing step for DMAP removal. When such strategy was followed, around 80−90% of DMAP was removed from **PBI-TA**.

In the case of **PBI-TB**, in the first DCM washing, only Meta was recovered (Table 2). The resulting salt of MPTS shows a poor solubility in this solvent and therefore remains precipitated with the adsorber, probably contributing to less than 1% of GTI contamination. The suggestion that the interaction between the GTI and **PBI-TB** comprises a chemical modification of the adsorber with hydrolysis of MPTS is coherent with the detection of GTI anion (*p*-toluenesulfonate) on MeOH washing solution, since this solvent is able to solubilize this compound. This observation was validated by coelution with a sample of *p*-toluenesulfonic acid (PTSA), presenting the same *p*-toluenesulfonate anion.

Since the API recovery steps are able to mitigate its loss without exceeding a target value of 7.5 mgGTI/gAPI, a possible API purification strategy can be sought with each adsorber targeting each impurity. Using **PBI-TA**, it is possible to remove DMAP and recover the API with a simple DCM washing step and to remove the bound impurity with a simple MeOH washing. Further regeneration of the adsorber could be performed with a HCl solution. In the case of **PBI-TB**, the adsorption step must take place at 50 °C to improve impurity removal. However, a simple DCM washing is enough to recover the API that was bound to the adsorber and reach the targeted values of 7.5 or 0.75 mg GTI/g API. For this polymer, a MeOH washing is able to remove the salt of the impurity, but its regeneration is impaired by the nature of the reaction between MPTS and the amine groups of the imidazole rings of the adsorber.

4. CONCLUSIONS

PBI-based adsorbers were obtained for the removal of impurities from API solutions in DCM. The polymer subjected to thermal treatment and acidic conditioning, **PBI-TA**, showed the best performance for removal of an aromatic amine, DMAP, with API losses lower than 10%. When the PBI is subjected to a basic treatment, the resulting adsorber, **PBI-TB**, shows improved performance to remove a sulfonate alkylating agent from solution with low API losses. However, in this case, the process requires improvement with temperature. The same adsorbers formulated as fibers showed a similar performance in API purification strategies, opening the way to several possibilities for separation processes based on filtration in organic solvent matrices using the fibers. In the case of both types of impurities, the final ratios of mg GTI/g API obtained were within the limits imposed by the TTC in the case of the API studied, Meta.

■ ASSOCIATED CONTENT

Supporting Information

The Supporting Information is available free of charge on the ACS Publications website at DOI: 10.1021/acs.iecr.9b01285.

DMAP and MPTS binding for 100, 1000, and 5000 ppm solutions in DCM for different PBI adsorbers; binding of DMAP in PBI-TA and MPTS in PBI-TB for 1000 ppm

DOI: 10.1021/acs.iecr.9b01285
Ind. Eng. Chem. Res. 2019, 58, 10524−10532

solutions in several solvents; SEM images of PBI polymer particles and fibers; illustrative histogram of the diameter distribution for electrospun fibers; adsorption binding isotherm physical parameters for DMAP, MPTS, and Meta for PBI-TA and PBI-TB at room temperature; kinetic physical parameters for DMAP and PBI-TA at room temperature and MPTS and PBI-TB at 50 °C; pseudo-second-order kinetic fitting models for DMAP and MPTS for 100 and 1000 ppm at room temperature; pseudo-second-order kinetic physical parameters obtained for DMAP and MPTS for 100 and 1000 ppm at room temperature (PDF)

AUTHOR INFORMATION

Corresponding Author

*Tel: +351 218419598; E-mail: frederico.ferreira@tecnico.ulisboa.pt.

ORCID

Carlos A. M. Afonso: 0000-0002-7284-5948

Frederico Castelo Ferreira: 0000-0001-5177-6237

Author Contributions

The manuscript was written through contributions of all authors. All authors have given approval to the final version of the manuscript.

Notes

The authors declare no competing financial interest.

ACKNOWLEDGMENTS

The authors acknowledge dedicated funding from Fundação para a Ciência e Tecnologia (FCT) through the Project SelectHost (PTDC/QEQ-PRS/4157/2014), iBB-Institute for Bioengineering and Biosciences (UID/BIO/04565/2013), UID/DTP/04138/2013, from Programa Operacional Regional de Lisboa 2020 (Lisboa-01-0145-FEDER-007317), and from Conselho Nacional de Desenvolvimento Científico e Tecnológico (CNPq-Brasil, 205201/2014-8). We thank Hovione PharmaScience Ltd. for supplying the APIs and technical know how. We also acknowledge Dr. Isabel Nogueira, from MicroLab (IST), for performing SEM experiments.

REFERENCES

(1) Zhou, L.; Mao, B.; Reamer, R.; Novak, T.; Ge, Z. Impurity Profile Tracking for Active Pharmaceutical Ingredients: Case Reports. *J. Pharm. Biomed. Anal.* **2007**, *44*, 421−429.

(2) Teasdale, A.; Elder, D.; Chang, S. J.; Wang, S.; Thompson, R.; Benz, N.; Sanchez Flores, I. H. Risk Assessment of Genotoxic Impurities in New Chemical Entities: Strategies to Demonstrate Control. *Org. Process Res. Dev.* **2013**, *17*, 221−230.

(3) Székely, G.; Amores de Sousa, M.; Gil, M.; Castelo Ferreira, F.; Heggie, W. Genotoxic Impurities in Pharmaceutical Manufacturing: Sources, Regulations, and Mitigation. *Chem. Rev.* **2015**, *115*, 8182−8229.

(4) EMEA Guidelines on Limits on Genotoxic Impurities.*EMEA/CHMP/QWP/251344/2006*; EMEA, 2006

(5) *Guidance for Industry Genotoxic and Carcinogenic Impurities in Drug Substances and Products: Recommended Approaches*; U.S. Department of Health and Human Services; Food and Drug Administration; Center for Drug Evaluation and Research (CDER), Dec 2008.

(6) Teasdale, A. *Genotoxic Impurities: Strategies for Identification and Control*; John Wiley & Sons: Hoboken, NJ, 2010.

(7) Buonomenna, M. G.; Bae, J. Organic Solvent Nanofiltration in Pharmaceutical Industry. *Sep. Purif. Rev.* **2015**, *44*, 157−182.

(8) Székely, G.; Gil, M.; Sellergren, B.; Heggie, W.; Ferreira, F. C. Environmental and Economic Analysis for Selection and Engineering Sustainable API Degenotoxification Processes. *Green Chem.* **2013**, *15*, 210−225.

(9) Székely, G.; Bandarra, J.; Heggie, W.; Sellergren, B.; Ferreira, F. C. Organic Solvent Nanofiltration: a Platform for Removal of Genotoxins from Active Pharmaceutical Ingredients. *J. Membr. Sci.* **2011**, *381*, 21−33.

(10) Esteves, T.; Ferreira, F. A.; Pina, M.; Bandarra, J.; Ferreira, F. C. Screening Commercial Available Resins for Simultaneous Removal of Two Potential Genotoxins from API Methanolic Streams. *Sep. Sci. Technol.* **2018**, 1.

(11) Esteves, T.; Viveiros, R.; Bandarra, J.; Heggie, W.; Casimiro, T.; Ferreira, F. C. Molecularly Imprinted Polymer Strategies for Removal of a Genotoxic Impurity, 4-dimethylaminopyridine, from an Active Pharmaceutical Ingredient Post-reaction Stream. *Sep. Purif. Technol.* **2016**, *163*, 206−214.

(12) Székely, G.; Bandarra, J.; Heggie, W.; Ferreira, F. C.; Sellergren, B. Design, Preparation and Characterization of Novel Molecularly Imprinted Polymers for Removal of Potentially Genotoxic 1,3-diisopropylurea from API Solutions. *Sep. Purif. Technol.* **2012**, *86*, 190−198.

(13) Heggie, W. Process for the Preparation of Mometasone Furoate. US 6177560 B1, 2001.

(14) Peeva, L.; Burgal, J. S.; Valtcheva, I.; Livingston, A. G. Continuous Purification of Active Pharmaceutical Ingredients Using Multistage Organic Solvent Nanofiltration Membrane Cascade. *Chem. Eng. Sci.* **2014**, *116*, 183−194.

(15) Székely, G.; Valtcheva, I. B.; Kim, J. F.; Livingston, A. G. Molecularly Imprinted Organic Solvent Nanofiltration Membranes − Revealing Molecular Recognition and Solute Rejection Behavior. *React. Funct. Polym.* **2015**, *86*, 215−224.

(16) Kim, J. F.; Székely, G.; Valtcheva, I. B.; Livingston, A. G. Increasing the Sustainability of Membrane Processes Through Cascade Approach and Solvent Recovery − Pharmaceutical Purification Case Study. *Green Chem.* **2014**, *16*, 133−145.

(17) Valtcheva, I. B.; Kumbharkar, S. C.; Kim, J. F.; Bhole, Y.; Livingston, A. G. Beyond Polyimide: Crosslinked Polybenzimidazole Membranes for Organic Solvent Nanofiltration (OSN) in Harsh Environments. *J. Membr. Sci.* **2014**, *457*, 62−72.

(18) Vicente, A. I.; Esteves, T.; Afonso, C. A. M.; Ferreira, F. C. Solvent Compatible Polymer Functionalized with Adenine, a DNA Base, for API Degenotoxification: Preparation and Characterization. *Sep. Purif. Technol.* **2017**, *179*, 438−448.

(19) Esteves, T.; Vicente, A. I.; Ferreira, F. A.; Afonso, C. A. M.; Ferreira, F. C. Mimicking DNA Alkylation: Removing Genotoxin Impurities from API Streams with a Solvent Stable Polybenzimidazole-Adenine Polymer. *React. Funct. Polym.* **2018**, *131*, 258−265.

(20) Haro Dominguez, P.; Grygiel, K.; Weber, J. Nanostructured Poly(benzimidazole) Membranes by N-alkylation. *eXPRESS Polym. Lett.* **2014**, *8*, 30−38.

(21) Rahimi, M.; Vadi, M. Langmuir, Freundlich and Temkin Adsorption Isotherms of Propranolol on Multi-Wall Carbon Nanotube. *J. Mod. Drug Discovery Drug Delivery Res.* **2014**, V1I3.

(22) Ho, Y. Selection of Optimum Sorption Isotherm. *Carbon* **2004**, *42*, 2115−2116.

(23) Qiu, H.; Lv, L. V.; Pan, B.; Zhang, Q.; Zhang, W.; Zhang, Q. Critical Review in Adsorption Kinetic Models. *J. Zhejiang Univ., Sci., A* **2009**, *10*, 716−724.

(24) Ho, Y.; Ofomaja, A. E. Pseudo-second-order Model for Lead Ion Sorption from Aqueous Solutions onto Palm Kernel Fiber. *J. Hazard. Mater.* **2006**, *129*, 137−142.

(25) Canadas, R. F.; Cavalheiro, J. M. B. T.; Guerreiro, J. D. T.; de Almeida, M. C. M. D.; Pollet, E.; da Silva, C. L.; da Fonseca, M. M. R.; Ferreira, F. C. Polyhydroxyalkanoates: WasteGlycerol Upgrade Into Electrospun FibrousScaffolds for StemCellsCulture. *Int. J. Biol. Macromol.* **2014**, *71*, 131−140.

(26) Pu, H. *Polymers for PEM Fuel Cells*; John Wiley and Sons: Hoboken, NJ, 2014.

DOI: 10.1021/acs.iecr.9b01285
Ind. Eng. Chem. Res. 2019, 58, 10524−10532

(27) Li, Q.; Jensen, J. O. *Membranes for Energy Conversion*; Wiley-VCH: Weinheim, 2008; Vol. 2.
(28) Scudder, P. H. *Electron Flow in Organic Chemistry: A Decision-Based Guide to Organic Mechanisms*; John Wiley & Sons: Hoboken, NJ, 2013.
(29) Valtcheva, I. B.; Marchetti, P.; Livingston, A. G. Crosslinked Polybenzimidazole Membranes for Organic Solvent Nanofiltration (OSN): Analysis of Crosslinking Reaction Mechanism and Effects of Reaction Parameters. *J. Membr. Sci.* **2015**, *493*, 568−579.
(30) Li, H.; Liu, Y. Polyelectrolyte Composite Membranes of Polybenzimidazole and Crosslinked Polybenzimidazole-polybenzoxazine Electrospun Nanofibers for Proton Exchange Membrane Fuel Cells. *J. Mater. Chem. A* **2013**, *1*, 1171−1178.
(31) Jahangiri, S.; Aravi, I.; Işıkel Şanlı, L.; Menceloğlu, Y. Z.; Özden-Yenigün, E. Fabrication and Optimization of Proton Conductive Polybenzimidazole Electrospun Nanofiber Membranes. *Polym. Adv. Technol.* **2018**, *29*, 594−602.
(32) Ki, C. S.; Gang, E. H.; Um, I. C.; Park, Y. H. Nanofibrous Membrane of Wool Keratose/Silk Fibroin Blend for Heavy Metal Ion Adsorption. *J. Membr. Sci.* **2007**, *302*, 20−26.
(33) Park, M. J.; Nisola, G. M.; Vivas, E. L.; Limjuco, L. A.; Lawagon, C. P.; Seo, J. G.; Kim, H.; Shon, H. K.; Chung, W. J. Mixed Matrix Nanofiber as a Flow-Through Membrane Adsorber for Continuous Li^+ Recovery from Seawater. *J. Membr. Sci.* **2016**, *510*, 141−154.

DOI: 10.1021/acs.iecr.9b01285
Ind. Eng. Chem. Res. 2019, 58, 10524−10532